Journal of
Nanoscience and Nanotechnology
Vol. 11, 9345–9356, 2011

REVIEW

The Research Progress of Quantum Dot Lasers and Photodetectors in China

Peng-Fei Xu[1], Hai-Ming Ji[1], Tao Yang[1,*], Bo Xu[1], Wen-Quan Ma[2], and Zhanguo Wang[1]

[1] Key Laboratory of Semiconductor Materials Science, Institute of Semiconductors, Chinese Academy of Sciences, Beijing 100083, People's Republic of China
[2] Nano-Optoelectronics Laboratory, Institute of Semiconductors, Chinese Academy of Sciences, Beijing 100083, People's Republic of China

Self-assembled In(Ga)As/GaAs quantum dots (QDs), known as "artificial atoms" for their fully quantized electronic states, show unique physical properties and new prospects for applications. Based on the QDs, an increasing number of leading laboratories on the world engage in developing novel optoelectronic devices with special advantages over existing devices. This paper reviews the current research developments in self-assembled QD devices in China, covering QD lasers and inter sublevel QD photodetectors. QD devices in China are undergoing a rapid advance and have achieved the world's best results in terms of certain characteristics.

Keywords: Quantum Dot, Lasers, Photodetectors.

CONTENTS

1. Introduction 9345
1.1. 0.94–1.16 μm QD Lasers 9345
1.2. QD Lasers in the Visible Range 9347
1.3. 1.3 μm QD Lasers 9347
1.4. 1.55 μm QD Lasers 9350
1.5. Quantum-Wire Lasers 9351
1.6. QD Photodetectors 9352
2. Conclusion 9355
Acknowledgment 9355
References and Notes 9355

1. INTRODUCTION

As the geometries in all three dimensions are comparable to the de Broglie wavelength of electrons, quantum dot (QD) is an ultimate quantum confined structure and the resulting electron energy levels are discrete, similar in the atomic physics.[1,2] The unique δ-function like density of states enables both new physics and novel device applications. Since the 1980s, a variety of methods have been tried to realize the semiconductor heterostructures that can provide carrier confinement and behave as electronic QD.[3] Little progress had been made until epitaxial growth of self-organized QDs was adopted. Stranski-Krastanow (SK) growth occurs in strongly lattice-mismatched systems where three-dimensional islands form spontaneously above a certain critical thickness to reduce the mismatch strain.[4] Devices based on these defect-free QDs have been extensively investigated worldwide and have presented amazing performance.[5–9]

Study on QD devices in China began in the mid-1990s. After researchers from Institute of Semiconductors, Chinese Academy of Sciences (CAS) made the first pulsed operation of QD laser diode (LD) operating at room temperature (RT),[10] QD lasers with different emission wavelengths as well as various performances such as low threshold current, high output power and high modulation rate have been developed.[11–25] On the other hand, QD inter sublevel photodetectors have been conceived and demonstrated since 1996, when Dr. Pan observed for the first time normal incident infrared absorption from a InGaAs/GaAs QD superlattice.[26–29] All of these QD devices are reviewed in this paper.

1.1. 0.94–1.16 μm QD Lasers

Since the emission of In(Ga)As/GaAs QDs is usually around 0.98 μm, lasers of this wavelength were the first breakthrough. As early as 1996, RT pulsed mode lasing of QD-LDs was demonstrated by the researchers from the Institute of Semiconductors, CAS, with an emission wavelength of $\sim$1 μm and threshold current density of 590A/cm^2.[10] Since 1997, RT-CW QD-LDs with low threshold current density and high output power have been successfully realized and their performance has gradually

*Author to whom correspondence should be addressed.

1533-4880/2011/11/9345/012 doi:10.1166/jnn.2011.5310

improved. In order for high power lasers to work reliably under high injection current, misfit dislocation defects from the large strains around the QDs should be significantly suppressed. CAS researchers introduced an InGaAs strain-reducing layer above each QD layer, which was first reported in the QD-LDs of ~1 μm wavelength, and they found that the lifetime of the devices was greatly improved in contrast to the QD-LDs without strain-reducing layers. Lifetime of more than 3760 hours under 0.6 W RT-CW operation was achieved for QD-LDs having RT-CW

Peng-Fei Xu received his BS degree from Southeast University, Nanjing, China, in 2007. Now he is pursuing his Ph.D. degree in Institute of Semiconductors, Chinese Academy of Sciences. His research interest has been in the area of semiconductor nanostructure growth, devices fabrication and their characterization.

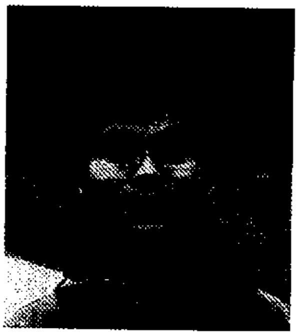

Hai-Ming Ji received BS degree from Fudan University, Shanghai and Ph.D. degree from Institute of Semiconductors, Chinese Academy of Sciences, Beijing in 2005 and 2010, respectively. In 2010 he joined Institute of Semiconductors, Chinese Academy of Sciences as an Assistant Researcher. His current research interests are MBE and MOVPE growth of InAs quantum dots on GaAs and InP substrates as well as related laser devices.

Tao Yang earned his Ph.D. in materials science and engineering from the University of Tokushima, Tokushima, Japan, in 1997. Since then, he joined the Central Research Lab., Hitachi Ltd., Tokyo, where he engaged in the development of blue nitride semiconductor lasers. In 2000, he moved to the New Energy and Industrial Technology Development Organization (NEDO), Tokyo, Japan, where he was devoted to developing the ultrafast optical technology based on semiconductor quantum dots (QDs) and photonic crystals, and then to the University of Tokyo in December, 2002, where he worked at the development of high-performance self-assembled InAs/GaAs QDs by MOCVD for lasers operating at 1.3 μm. From 2006, he became a professor at the Institute of Semiconductors, Chinese Academy of Sciences (CAS), Beijing, China. His present research interest focuses on the growth and characterization of low-dimensional semiconductor heterostructures including QDs and quantum wells by MBE or MOCVD as well as their applications in various devices such as lasers, detectors, solar cells, etc. Professor Yang has authored/co-authored more than 50 peer-reviewed scientific publications and more than 40 internal conference papers. He has 7 patents granted or pending. He was awarded the NEDO fellowship in 2000 and the "Hundred Talent Program" of CAS in 2007, respectively.

Bo Xu graduated from the University of Science and Technology of China in 1989, and got his Master degree in the Institute of Semiconductors, Chinese Academy of Sciences in 1992. Since then, he worked in the Institute of Semiconductors on molecular beam epitaxy growth of low-dimensional semiconductor materials. He conducted research on high-mobility two-dimensional electron gas materials from 1992 to 1994, and on high-power quantum-well laser diodes (LDs) from 1995 to 2000. Since 2001, he focused on the controlled growth of strain-induced self-assembled quantum-dot (QD) and quantum-wire (QWR) materials, and their application in semiconductor quantum devices, such as high-power QD-LDs, GaAs-based 1.3 μm QD-LDs and InP-based QWR-LDs. He has author/co-authored more than 30 journal publications and conference presentations.

REVIEW

Wen-Quan Ma got Ph.D. from Humboldt University in 2001 and his Ph.D. thesis work was preformed in Paul Drude Institute for Solid State Electronics, BerlinGermany. He joined Institute of Semiconductors, Chinese Academy of Sciences (CAS) in October 2004, and became a gainer of the "Hundred Talents Program" of CAS in 2005. Dr. Ma has been working on growth, characterization and device investigation of low dimensional semiconductor nanostructures. His current research area includes antimonide based material growth and device applications, quantum dot infrared photodetector, and self-organized growth of lateral ordered semiconductor nanostructures by molecular beam epitaxy.

Zhanguo Wang (Z. G. Wang) graduated from the Department of Physics, Nankai University, in 1962. Then he immediately joined the Institute of Semiconductors, Chinese Academy of Sciences (IS, CAS), engaged in studies on semiconductor materials physics and materials characterization till 1980. From 1980 to 1983, he was a visiting scientist at the Department of Solid State Physics, the University of Lund, Sweden, working on photoluminescence and deep levels of semiconductors. By the end of 1983 he became are search professor and a head of Semiconductor Materials Division of IS, CAS in 1986. From 1990, Professor Wang served as director of Key Laboratory of Semiconductor Materials Science and a deputy director of the IS, CAS, vice president of Chinese Materials Research Society and director of Semiconductor and Integration Technology Society, the Chinese Institute of Electronics etc. From 1984 to 1993, he conducted research mainly in the space GaAs crystal growth and characterization, GaAs and InP based super lattice, quantum well structures, MBE growth and its property studies. From 1994 till now, his research work has concentrated to low dimensional semiconductor nanostructures growth and quantum devices fabrication. He has published 3 books and more than 180 refereed papers in many authoritative journals. Professor Wang was elected as a member of the CAS in 1995.

peak output power of 3.6 W and threshold current density as low as 220A/cm^2, as shown in Figures 1 and 2, respectively.[11,12] These QD-LDs were used to make a fiber-coupled high-power LD module with an output power of ≥10 W. Up to now, the QD-LDs working in RT-CW mode at ~1 μm wavelength show a maximum output power of 4.15 W from the 100 μm-wide front facet, with threshold current density around 120 A/cm^2 and lifetime of more than 5000 hours at 1 W.

On the other hand, because of the broad gain profile of the QDs Yang et al. demonstrated QD lasing lines covering the wavelength window as wide as 26 nm at 20 °C and 52 nm at 80 K, which is highly desirable for making widely tunable lasers.[13]

1.2. QD Lasers in the Visible Range

InAs QDs in GaAs matrices mostly emit in the near infrared range. In order to extend the spectrum range of the QDs into the visible range, InAlAs QDs in AlGaAs matrices should be used instead. In this material system, many issues related to the severe O contamination during the MBE growth of high Al content layers need to be managed. By optimization of structural parameters and growth conditions, researchers from the Institute of Semiconductors CAS and their colleagues showed QD-LDs lasing in the red-light range. The devices can operate in CW mode at low temperatures (≤ 220 K) with threshold current density of ~400 A/cm^2 at 78 K, and in pulsed mode at RT. The emission wavelength is between 700~750 nm. It was also demonstrated that the lasing came from the ground-state transition of the InAlAs/AlGaAs QDs.[14]

1.3. 1.3 μm QD Lasers

Another widely investigated emission band of the QD lasers lies in a window at 1.3 μm which has significant

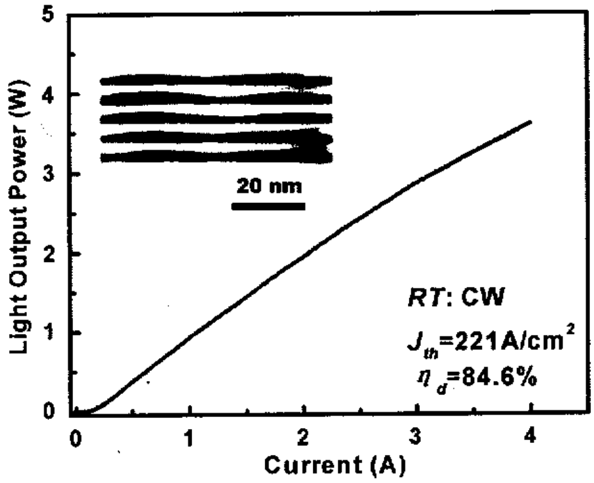

Fig. 1. Output power from both uncoated facets vs injection current of a high-power QD-LD in RT-CW mode. The inset shows the cross-sectional TEM image of the QD layers in the active region. Reprinted with permission from [12], H. Y. Liu et al., *Appl. Phys. Lett.* 79, 2868 (**2001**). © 2001, American Institute of Physics.

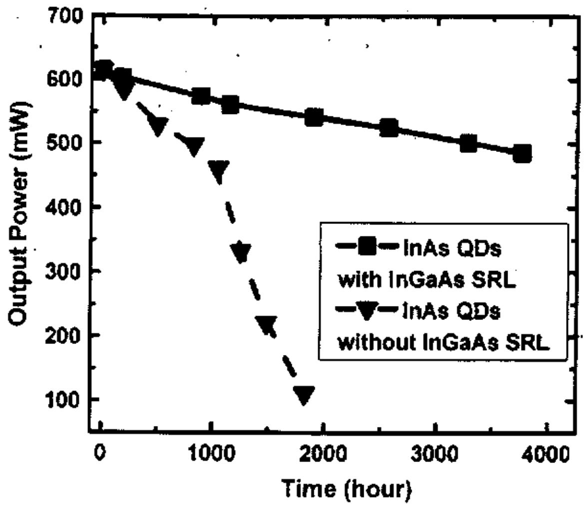

Fig. 2. Output power (from the uncoated front facet) as a function of the aging time of a high-power QD-LD in RT-CW mode with strain reducing layers, compared to another QD-LD without strain reducing layers. Reprinted with permission from [12], H. Y. Liu et al., *Appl. Phys. Lett.* 79, 2868 (**2001**). © 2001, American Institute of Physics.

potential in optical communication.[15–19] The QD lasers offer lower threshold current density, improved temperature stability and a broader modulation band than their conventional quantum well counterparts. The QD laser structures were grown by molecular-beam epitaxy (MBE), and the lasers based on the structures were fabricated by standard photolithography and wet etching. Fabry-Pérot lasers with broad areas and narrow stripes have been made to investigate material and device characteristics of the QD lasers.

Before starting to present the performances of the 1.3 μm self-assembled InAs/GaAs QD lasers, the structural and optical characteristics of the optimum QDs grown by MBE are briefly introduced. Figure 3 shows a surface image for a single layer of InAs QDs deposited on a GaAs substrate at 485 °C, measured in an area of 1×1 μm^2 by atom force microscopy (AFM). From the measurement, the areal density of the QDs is typically 4.0×10^{10} cm^{-2}, and the average height and base diameter of the QDs are about 6 nm and 30 nm, respectively. Figures 4 and 5 show the corresponding photoluminescence (PL) spectra from the QDs, obtained respectively at low (15 K) and room temperatures. The QD ensemble has been covered by a 6-nm-thick $In_{0.17}Ga_{0.83}As$ strain-reducing layer (SRL) and a 100-nm-thick GaAs capping layer in order to perform the PL measurements. A full width at half max(FWHM) of about 26.3 meV is obtained under a low excitation power of about 50 mW from the low-temperature PL measurement, as shown in Figure 4, which demonstrates the high uniformity of the InAs QDs. Furthermore, the FWHM at RT, as shown in Figure 5, is close to that obtained at the low temperature, which further indicates that the QDs are highly uniform.[30] In addition the PL peak at RT is located at 1.31 μm, as shown in Figure 5. To increase the density of QDs, multi-layer structures of QDs have been fabricated, where the QD layers are separated by a 6-nm-thick $In_{0.17}Ga_{0.83}As$ SRL and a 35-nm-thick GaAs layer. Figure 6 shows the RT-PL spectra from the structures with different QD layers, where the PL peak intensity increases as the stacking number increases, due to the increase of QD density with stacking. This shows that the multi-layer structures are of high quality.

Based on the optimized QD growth above, lasers of five stacked InAs QD layers in the active region were fabricated. From the relationship between the reciprocal external differential quantum efficiency and the cavity, a saturation modal gain as high as of 17.5 cm^{-1}, an internal quantum efficiency of 62.6% and an internal loss of 2.7 cm^{-1} have been derived for the 1.3 μm QD

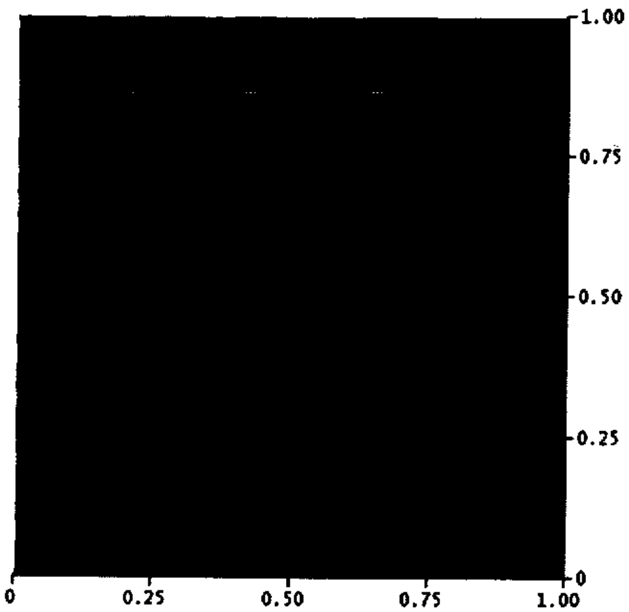

Fig. 3. Surface AFM image of optimum InAs quantum dots grown on GaAs by MBE, measured in a 1×1 μm^2 area.

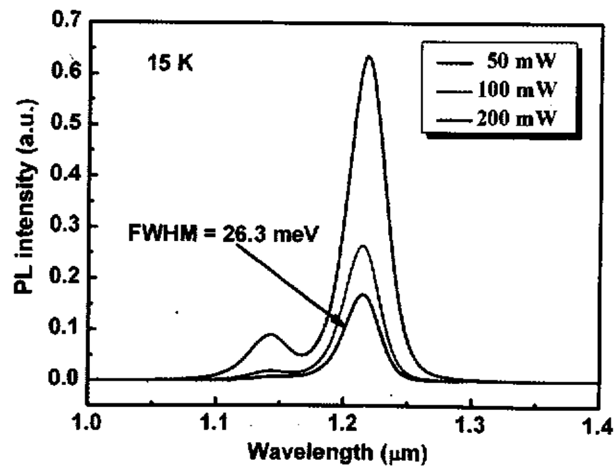

Fig. 4. PL spectra from the single layer of InAs/GaAs QDs, obtained under different excitation powers at 15 K. The state filling effect can be observed with increasing excitation powers.

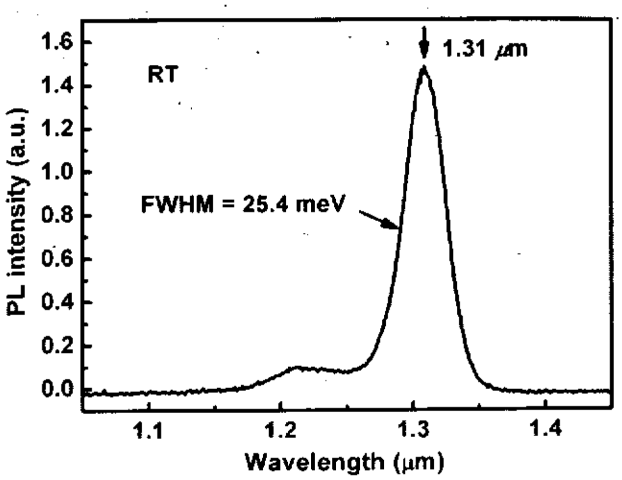

Fig. 5. Corresponding PL spectrum from the single layer of InAs/GaAs QDs at RT.

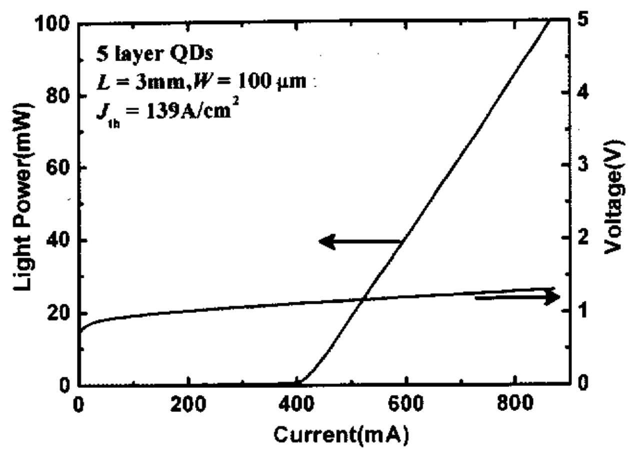

Fig. 7. *P–I* and *V–I* characteristic for a broad area QD laser with a cavity length of 3 mm, measured under pulse bias at RT.

lasers.[17] In particular, a threshold current density as low as 139 A/cm^2 was achieved for the QD lasers with a ridge width of 100 μm and a cavity length of 3 mm, as shown in Figure 7. This corresponds to a threshold current densityof 27.8 A/cm^2 per layer. For modulation operation, narrow waveguide lasers with short cavity lengths were fabricated. Furthermore, paddle-electrodes on the *p*-doped cladding-layer sides were adopted to reduce the parasitic capacitance. In addition, high-reflectivity coatings (95% and 60%) were applied on both facets of the cavity. The QD laser with 4-μm-width and 600-μm-length shows a low threshold current of 5 mA, which enables a small bias current and a large dynamic range for the modulation applications. The RT lasing spectrum from the laser is around 1293 nm at an injection current of 6 mA. Figure 8 shows the large-signal responses under different modulation rates, measured at 25 °C.[18] Clear eye patterns can be seen. The extinction rations are 2.7 dB, 2.8 dB, and 2.3 dB for 2.5 Gb/s, 5 Gb/s and 10 Gb/s, respectively. Moreover, clear open eye patterns under the 10 Gb/s modulation

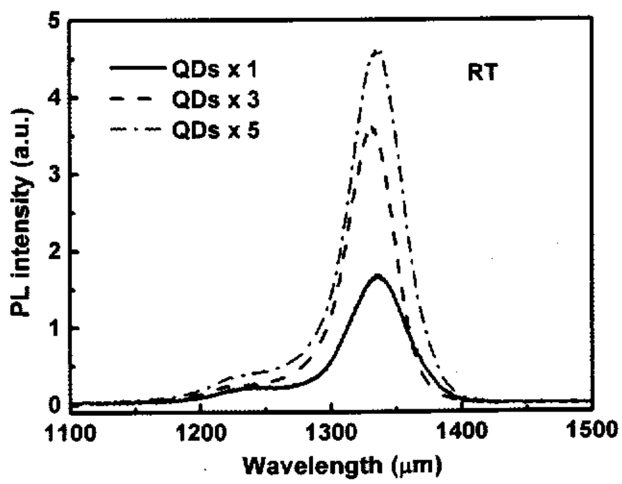

Fig. 6. RT spectra from 1, 3 and 5 stacked InAs/GaAs QD layers.

speed can be obtained at environmental temperatures of up to 50 °C, as shown in Figure 9. Finally, the latest study indicates that the excited state lasing of the QD has the potential in improving the modulation bandwidth due to an increase in the saturated gain and reduced carrier scattering time of the excited state compared to the ground state.[19]

Although the QD lasers are predicted to be temperature-insensitive, it is problematic to realize for the reason that the energy levels in the valence band are closely spaced and consequently the holes can be easily thermally broadened. To overcome this deficiency, *p*-type modulation doping in the QD active region has been proposed to keep the gain unchanged by providing plentiful holes.[31] Using this technique, researchers from Japan have demonstrated the first temperature-insensitive 1.3 μm QD lasers whose characteristic temperature reached 320 K in the temperature range from 20 to 60 °C.[32] The technique of *p*-type modulation doping was also studied here.[17] For comparison, QD lasers with and without *p*-type doping were fabricated. Figure 10 schematically illustrates the structure of our *p*-doped lasers, where Be-doping (5×10^{17} cm^{-3}) is introduced into a 5-nm-thick GaAs layer in the 40-nm-thick GaAs spacers and the doping layer is 10 nm away from the upper QD layers. Owing to the introduction of *p*-type doping impurities in the active region, there is a little degeneration in the internal quantum efficiency and the internal loss for *p*-type doped lasers compared to the undoped lasers.[17] However, the temperature stability of output can be greatly improved for the *p*-type doped lasers, due to the *p*-type modulation doping. Figures 11(a and b) show the *P–I* characteristics of the undoped and *p*-type doped lasers with a cavity length of 1200 μm, measured under pulse bias between 10 °C and 100 °C. Figures 12(a and b) present the corresponding temperature-dependent threshold current and slope efficiency in Figures 11(a and b). From Figure 11, it can be clearly seen that the excited state lasing for the undoped laser begins at a temperature

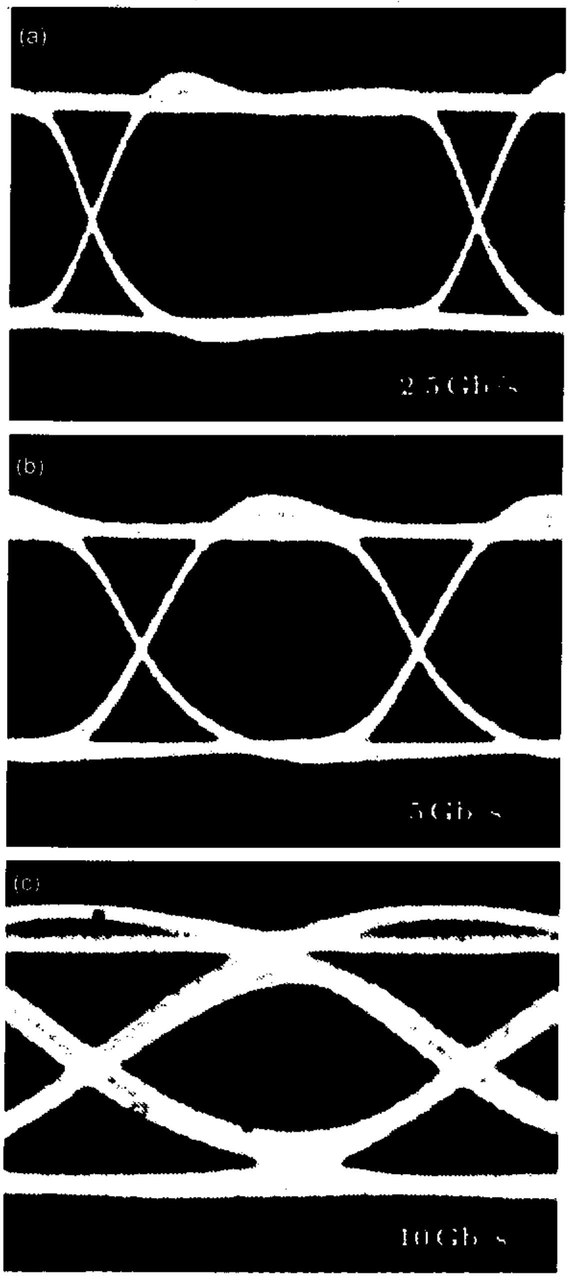

Fig. 8. Eye patterns under modulation rates of (a) 2.5 Gb/s, (b) 5 Gb/s, and (c) 10 Gb/s with a direct current bias of 60 mA, measured at 25 °C. Reprinted with permission from [18], H. M. Ji et al., *Chin. Phys. Lett.* 27, 034209 (**2010**). © 2010, Chinese Physical Society.

of 90 °C, where as it is inhibited for the whole measured temperature range in the *p*-doped laser. Furthermore, the characteristic temperature of the *p*-doped laser is increased to as high as 436 K in the temperature range from 10 to 60 °C, compared to 68 K of the undoped counterpart, as shown in Figure 12. Besides, by choosing appropriate facet coating to decrease the facet loss of the ground state meanwhile to increase that of the excited state, Cao et al. from CAS successfully delayed the excited state lasing and eventually improved the characteristic temperature of the QD lasers.[33]

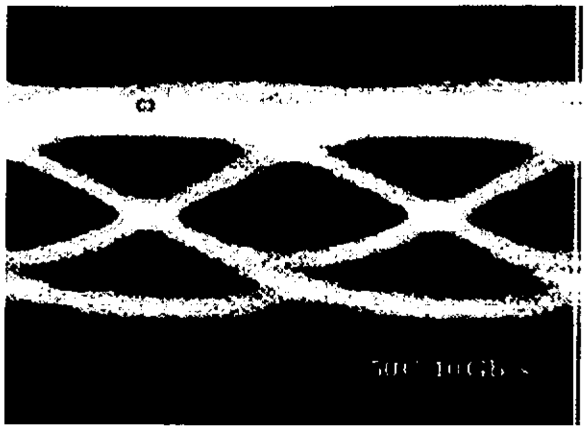

Fig. 9. Eye pattern under the 10 Gb/s modulation rate at the high environmental temperature of 50 °C. Reprinted with permission from [18], H. M. Ji et al., *Chin. Phys. Lett.* 27, 034209 (**2010**). © 2010, Chinese Physical Society.

1.4. 1.55 μm QD Lasers

InAs QDs on InP substrate have provided an effective way to obtain telecommunication wavelength, and can be adopted as active region in the semiconductor lasers for fiber-optic communication. To achieve the wavelength of 1.55 μm, particular procedures such as post-growth annealing,[34]GaAs or GaP inter layers between InAs QD layer and buffer layer etc.,[35,36] have been used widely in the epitaxy of InAs/InP QDs. Gong et al. from Shanghai Institute of Microsystem and Information Technology, CAS have demonstrated 1.55 μm InAs/InP QDs and QD lasers without the procedures mentioned above.[20] By only adjusting the deposition amount of InAs, InAs QDs with a density in the range of 10^{10} cm^{-2} and emission wavelengths around 1.55 μm have been achieved on InGaAsP barriers by gas-source MBE, as shown in Figure 13.

Based on this QD epitaxy technology, they also fabricated lasers of five-fold-stack InAs QDs in the active region. The lasers with a stripe width of 6 μm have a lasing wavelength centered at 1.556 μm, and a threshold current density for infinite cavity length is derived as low

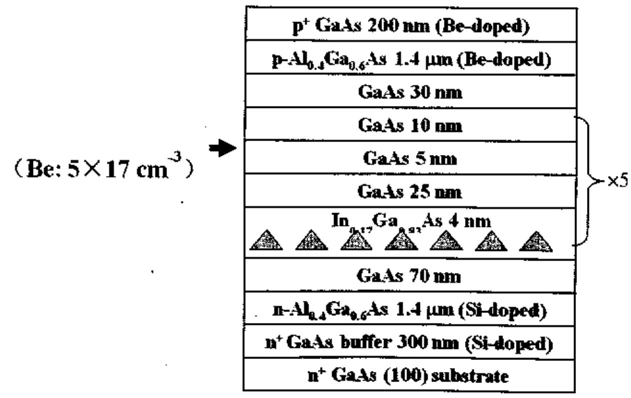

Fig. 10. Schematical cross-section illustration of the .structure of *p*-doped 1.3 μm InAs/GaAs QD lasers, grown by MBE.

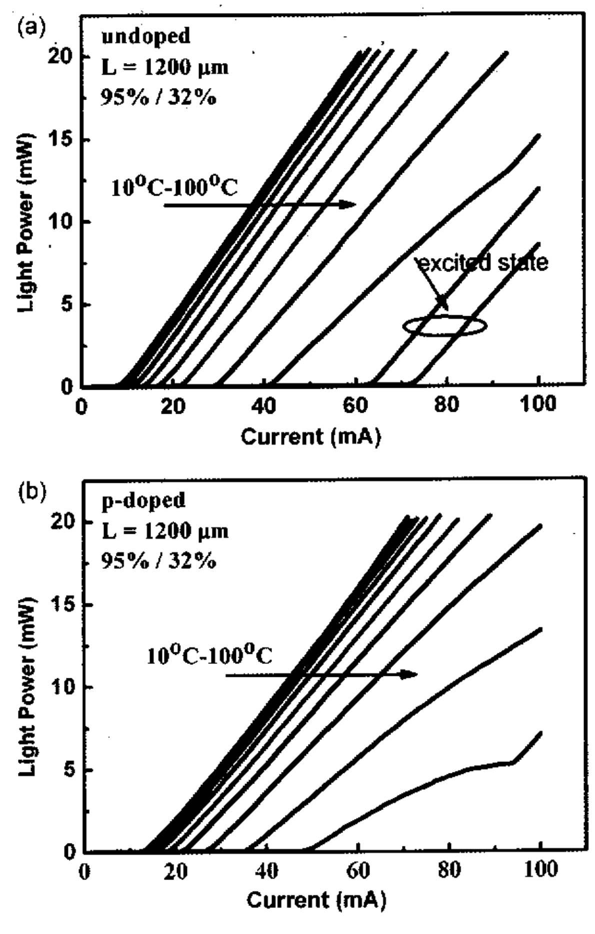

Fig. 11. (a and b) respectively show the P–I characteristics of ridge-waveguide undoped and p-type doped lasers with the cavity lengths of 1000 μm, measured under pulse bias from 10 °C to 100 °C.

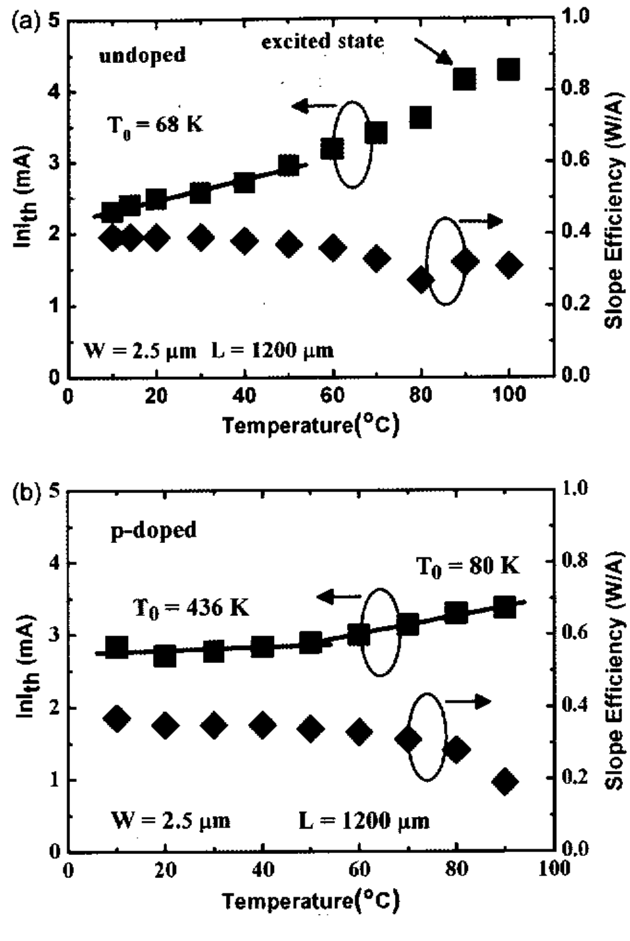

Fig. 12. Temperature dependence of threshold current and slope efficiency obtained from Figure 10.

as 638 A/cm^2, corresponding to about 128 A/cm^2 per QD layer, as shown in Figure 14. Moreover, a characteristic temperature as high as 69 K is derived in the temperature range of 20–70 °C from a device with a cavity length of 2 mm and as-cleaved facets.

An interesting lasing spectrum has been observed in their InAs/InP QD lasers, in which the lasing peak splitting occurred as the injected current increased, as shown in Figure 15.[21] Similar phenomena have been reported in monolithic mode-locked 1.55 μm InAs/InP QD lasers, and have been explained by Rabi oscillation.[37] However, Gong et al. have demonstrated that the dependence of splitting frequency of two peaks on the square root of the output power is nonlinear in their edge-emitting lasers. In this case, the model of Rabi oscillation is not suitable to explain the observed lasing spectrum. By comparison of the lasing spectra and EL spectra under the same injection levels, they suggested that the state-filling effect may be responsible for the lasing peak splitting and shifting.

1.5. Quantum-Wire Lasers

The morphology of strain-induced self-assembled InAs nanostructures grown on InP substrates has a large dependence much on the composition of buffer layer. For instance, InAs deposited on $In_{0.53}Ga_{0.47}$. As buffer layers lattice-matched to InP substrates often presents as quantum dots, while on $In_{0.52}Al_{0.48}$. As layers which are also lattice-matched to InP, elongated InAs nanostructures are frequently formed, lying in the growth plane along the [1–10] direction. Their width and height are usually in the 10 nm range, small enough to show quantum-confinement effects, but their length is much longer, in the range of 1 micron, so they are called quantum-wires (QWRs) or quantum-dashes. In the case of InAlGaAs buffer layers lattice-matched to InP, it depends on the Al/Ga ratio whether the InAs nanostructures take the form of nano-dots or nano-wires.

The researchers from the Institute of Semiconductors CAS have made extended studies on InAs nanostructures on InP substrates, and have found that in coupled multilayers of QWRs grown in InAlAs matrix, a wire in an upper layer tends to form in the interstice of the two wires in the lower layer, rather than just above the lower ones. Thus the wires in the multilayers show strong anti-correlation in the growth direction.[22,23] They have also tried to control the InAs morphology as QDs or QWRs

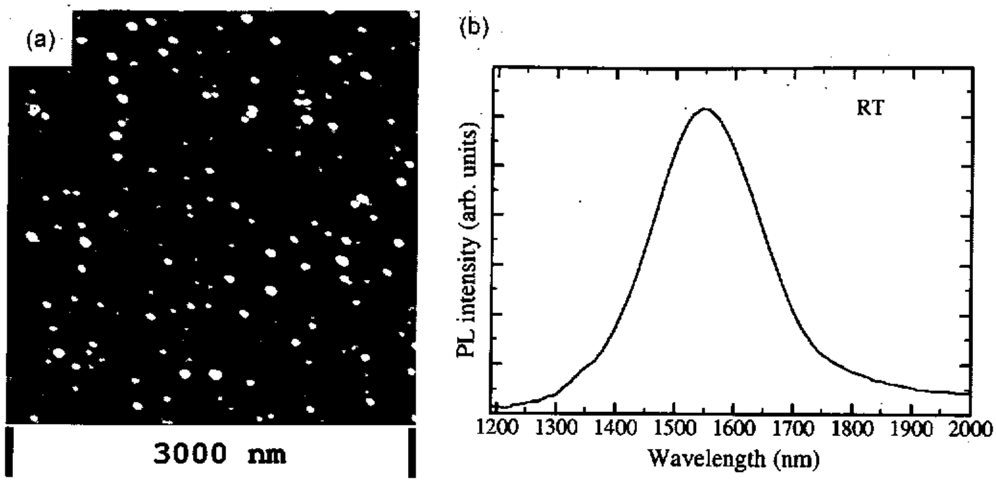

Fig. 13. AFM image of the InAs QDs on InGaAsP buffer and the RT photoluminescence of the QDs. Reprinted with permission from [20], S. G. Li et al., *Appl. Phys. Lett.* 93, 111109 (**2008**). © 2008, American Institute of Physics.

on InAlAs (as well as InAlGaAs) buffer layers lattice-matched to InP by adjusting As over pressure on the growth surface.[24]

On the basis of the controlling technique on InAs QWR growth, quantum-wire LDs with an emission wavelength around 1.7 μm were achieved on InP substrates.[25] The devices can work in the RT-CW mode, with output powers above 18 mW, as shown in Figure 16. It was also found that lasers with cavities along the [110] direction have lower threshold current densities than devices with cavities along the [1–10] direction, indicating the anisotropic nature of the quantum-wires in the laser's active region.

1.6. QD Photodetectors

The idea of a quantum dot infrared Photodetector (QDIP) was proposed in 1996 by Ryzhii.[38] Since then QDIP has attracted a large amount in interest. QDIP exhibits some advantages, such as operation under normal incidence infrared irradiation without fabricating surface gratings, and higher working temperature compared with quantum well infrared photodetector (QWIP). The former advantage is due to the three dimensional quantum confinements of electrons in the dots. This advantage makes the QDIP focal plane array (FPA) device fabrication easier and can lower the QDIP FPA cost. The latter is due to the electron lifetime in the inter subband transition being longer than that in the QWIP. However, although QDIP has the

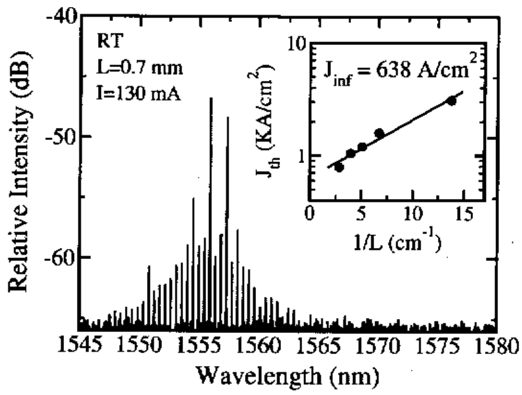

Fig. 14. RT lasing spectrum of a QD laser at 1.02 times threshold current. The inset is the threshold current density as a function of reciprocal cavity length. Reprinted with permission from [20], S. G. Li et al., *Appl. Phys. Lett.* 93, 111109 (**2008**). © 2008, American Institute of Physics.

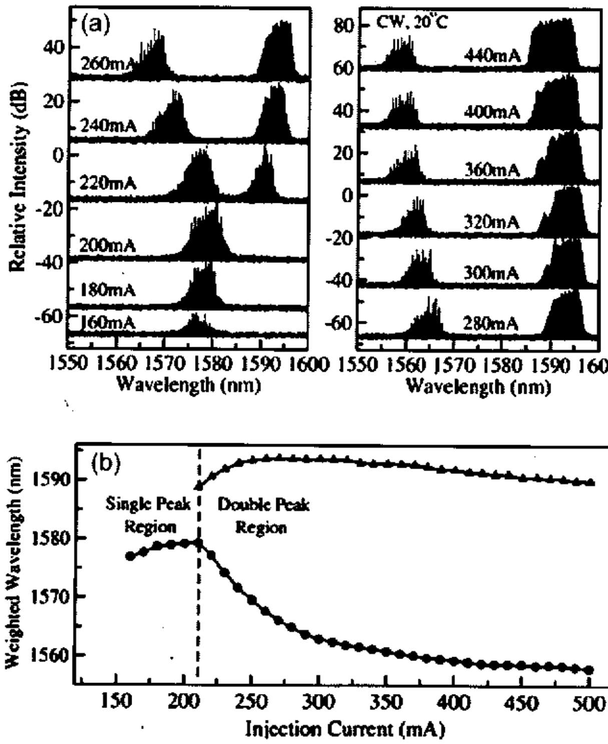

Fig. 15. (a) Lasing spectra of a QD laser with different injection currents at 20 °C. (b) The current dependence of the intensity weighted central wavelength of the lasing peaks. The single peak and double peak region are divided by the dashed line. Reprinted with permission from [21], S. G. Li et al., *Appl. Phys. Lett.* 95, 251111 (**2009**). © 2009, American Institute of Physics.

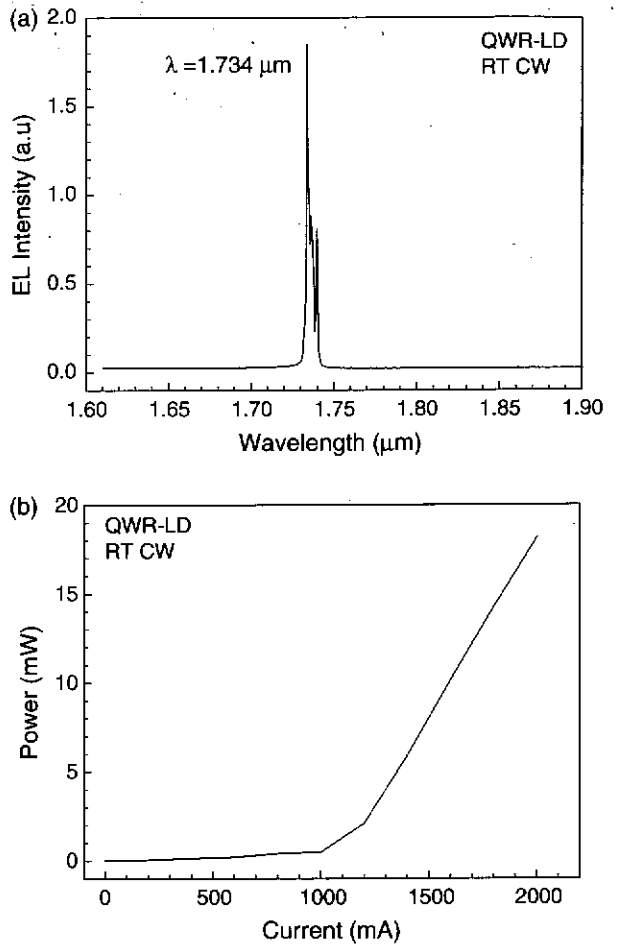

Fig. 16. (a) Lasing spectrum of a QWr-LD. (b) Output power versus injection current of the QWr-LD in RT-CW mode.

advantages mentioned above, the main hurdles hindering device performance of QDIP is related to the problem of achieving high quality QD fabrication. Concretely, one difficulty is the large size fluctuation of the QDs. The inhomogeneous broadening can weaken the absorption and therefore results in a low detectivity. This is not good for infrared detector applications. Another problem is that, although the absorption and the QDIP device have been achieved for normal incidence geometry, the inter subband absorption of the electrons in the dots for a normal incidence light is still very weak due to the fact that present SK dots have a very small height-to-width ratio of about 1:7. In other words, in order to enhance the absorption efficiency, the dot height-to-width ratio should be increased. Besides these points, some device scheme to suppress the dark current is also very desirable for the enhancement of the QDIP performance.

As mentioned above, one important aspect for QDIP device is to grow more uniform dots. A structure of (In, Ga)As/GaAs quantum dots is grown, which is vertically correlated and laterally aligned in a hexagonal way thus forming three-dimensionally ordered arrays by MBE.[27] The growth pathway is based on a self-assembly mechanism by strain-mediated multilayer vertical stacking on a planar GaAs(100) rather than on a prepatterned substrate by MBE. The strain energy of lateral island–island interaction is minimum for arrangement of the hexagonal ordering. However, realization of hexagonal ordering not only depends on a complicated tradeoff between lateral and vertical island–island interaction, but also is related to a delicate and narrow growth kinetics window. Figure 17(a) depicts the AFM image of the sample; the scanning area is $1.5 \times 5\ \mu m^2$. Figure 17(a) clearly demonstrates a distinctive lateral ordering of the QDs with an areal density of about 1×10^{10} cm^{-2}. However, it can be seen easily that the distribution of the QDs is different from the linear chains. In order to reveal the way of the lateral alignment of the QDs, Figure 17(b) shows the close-up of a small area of the AFM image marked as a white box in Figure 17(a). Four neighboring conventional surface unit cells are also marked as the hexagons in Figure 17(b). It is found that the dots are slightly elongated and are lined up along the [0-11] direction as chains, which are themselves nearly aligned along the two orthogonal directions [001] (or [00-1]) and [0-10]. In other words, the dots are aligned along both the [0-11] and [001] directions forming a hexagonal in-plane ordering. This hexagonal alignment can be seen very clearly from Figure 17(c), an image of the two dimensional (2D) fast Fourier transformation (FFT) of Figure 17(a). Except for the origin in the FFT image, the two bright spots in the [011] direction reflect that the [0-11]-oriented chains have a long range ordering across the [011] direction, while the other four spots located in the directions of [001], [0-10], [001], and [010],

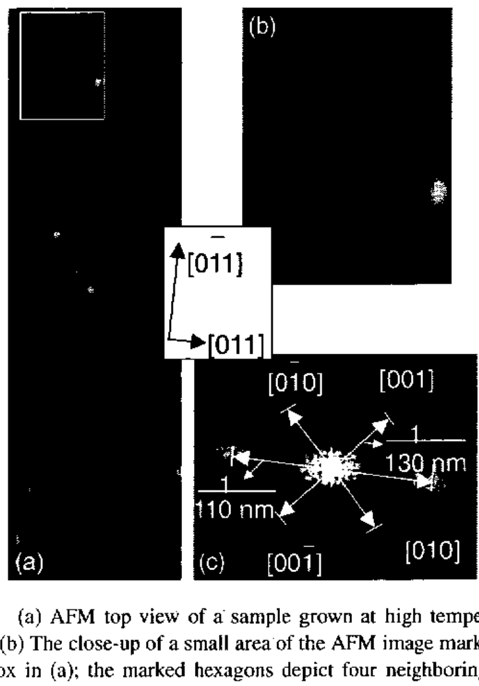

Fig. 17. (a) AFM top view of a sample grown at high temperature of 540 °C. (b) The close-up of a small area of the AFM image marked as the white box in (a); the marked hexagons depict four neighboring surface unit cells. (c) shows the 2D FFT image of AFM picture (a). Reprinted with permission from [27], W. Q. Ma et al., *Nanotechnology* 17, 5765 (2006). © 2006, Institute of Physics Publishing.

respectively, demonstrate a long range ordering of the dots along those directions. From Figure 17, the period of the chains along the [011] is 105 nm and that along the [001] ([0-10]) is 124 nm.

These hexagonal dots demonstrate enhanced absorption.[28] Figure 18 shows the absorption spectra of the ordered dots and the non-ordered dots. The ordered dots show a peak at around 11 μm while no clear normal incidence absorption peak was detected for non-ordered dots. To test if the Fourier transform infrared (FTIR) measurement for normal incidence geometry is correct, the researchers cut both the ordered and non-ordered dot samples in the same length and width and polished the cut piece 45° at the two edges and performed the FTIR under the waveguide geometry and the results are confirmed. The enhanced absorption of the ordered QD sample is probably due to the improved size uniformity; this is supported by the PL measurements. Since the inhomogeneous broadening can weaken the absorption, to reach the same level of absorption, a much larger number of QDs is required to compensate for the loss due to the size fluctuation.

In 2008, several types of InGaAs/GaAs QDIP devices fabricated by MBE were reported.[29] Figure 19 depicts the photocurrent spectra of the sample measured in normal incidence geometry at different applied biases at 77 K. For a small positive bias (by positive it means that the electrons transport from the top to the bottom), a peak in the photocurrent spectrum occurs at 5.5 μm; with increasing the bias voltage above 0.7 V, another peak at 7.0 μm appears while the 5.5 μm peak gradually decreases. Therefore, by tuning the applied bias in the positive direction, this QDIP device achieves a dual color detection function. In contrast, when the applied bias is negative, the 5.5 μm peak vanishes while the 7.0 μm peak remains, as can be seen from the spectrum shown in Figure 19, for the bias voltage at −1.0 V. For the 5.5 μm peak, the general trend is that the peak intensity diminishes with increasing the bias voltage. The very slight deviation from this trend between points at 0.5 V and 0.7 V (also between the points at 1.3 V and 1.5 V) might be due to the influence of the long tail of the 7.0 μm peak on the high energy side. In contrast, the 7.0 μm peak shows an ascending tendency with increasing positive bias. These features undoubtedly point out that the 7.0 μm peak is photoconductive while the 5.5 μm peak is intrinsically photovoltaic. Such a photovoltaic behavior is generally related to a breaking of the structural inversion symmetry. The 5.5 μm peak only appears for positive bias in this case. For photovoltaic QWIP, asymmetric structural design is usually employed. As a comparison, the self-assembled dots based on the SK growth mode intrinsically lack in inversion symmetry due to the existence of the wetting layer, the asymmetric shape of the dots, and even anisotropic strain distribution resulting in also a built-in electric field. Therefore, it is not surprising that such a photovoltaic behavior is observed. Figure 20 schematically illustrates the involved inter subband transitions of electron in the conduction band. It is proposed that the 5.5 μm peak arises from the transition of electron from the ground state E_0 to a continuum state of the QDs. Since the barrier thickness is finite, the energy states in the continuum should be also separate. For a symmetric quantum well structure, absorption is possible provided that the parity of wave function for the involved two states is different.

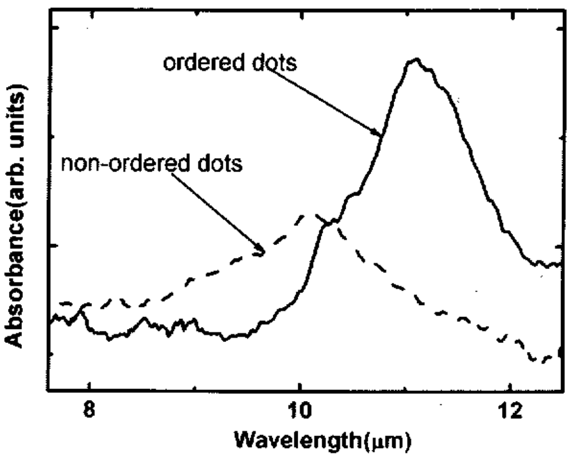

Fig. 18. RT absorption spectra under normal incidence geometry. Reprinted with permission from [28], W. Q. Ma et al., *Infrared Phys. & Technol.* 50, 162 (**2007**). © 2007, Elsevier.

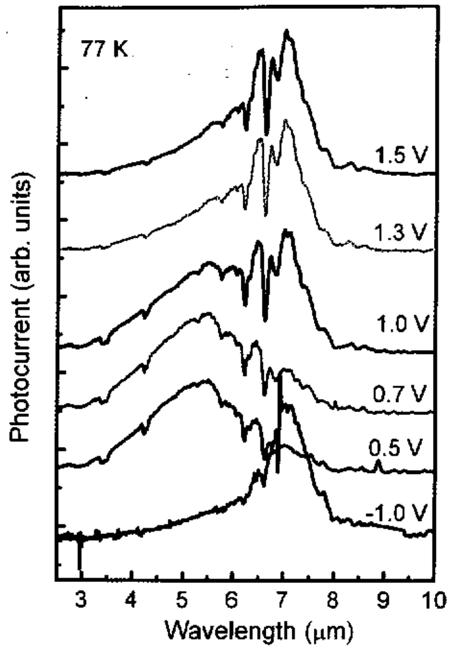

Fig. 19. Photocurrent spectra of the QDIP at different bias voltages measured in the normal incidence geometry at 77 K. Reprinted with permission from [29], W. Q. Ma et al., *Appl. Phys. Lett.* 93, 013502 (**2008**). © 2008, American Institute of Physics.

Figure 21 shows the photocurrent spectra of a dots-in-a-well structure, which has been widely employed.

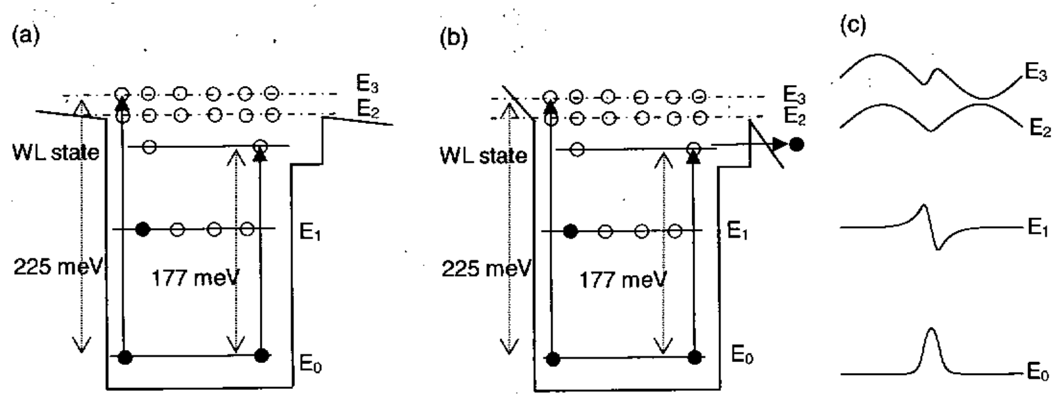

Fig. 20. Proposed conduction band diagram with the involved transitions in the QDIP for a small (a) and a large (b) positive bias voltage. E_0 and E_1 are the two bound states of the dots while E_2 and E_3 show the two separate continuum states; The closed circle shows a state occupied with an electron and the open circle corresponds to an empty state. (c) depicts the shapes of wave function for E_0, E_1, E_2 and E_3. Reprinted with permission from [29], W. Q. Ma et al., *Appl. Phys. Lett.* 93, 013502 (**2008**). © 2008, American Institute of Physics.

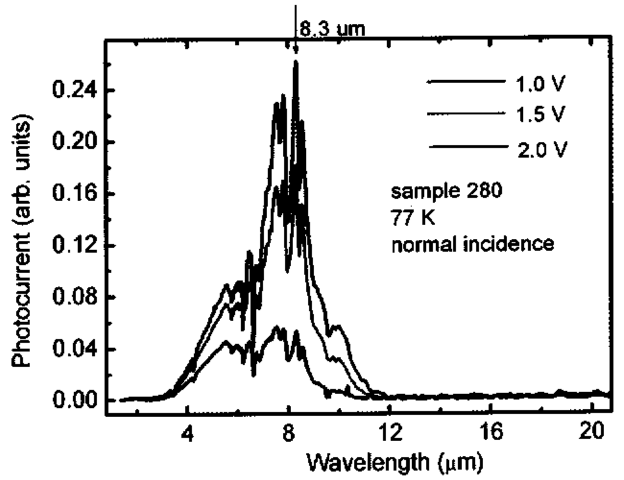

Fig. 21. Photocurrent spectra of the DWELL device under normal incidence geometry at 77 K.

The photoresponse of this device covers the long wavelength range and the response peak is 8.3 μm. One remarkable feature is that the peak responsivity reaches 8 A/W when the applied voltage is 4.5 V (see Fig. 22).

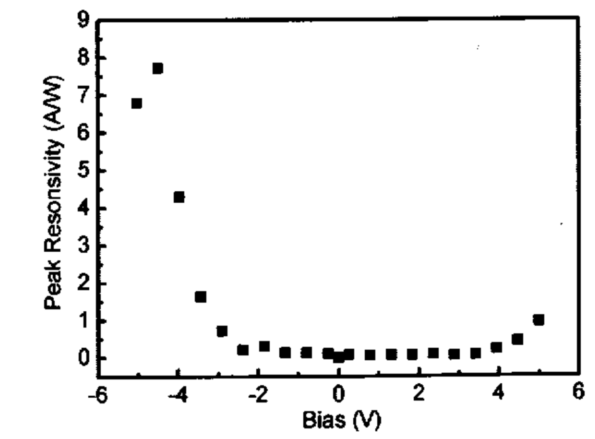

Fig. 22. Dependence of the peak responsivity on the applied bias voltages.

2. CONCLUSION

The excellent properties and potential applications of QD materials and devices have attracted wide attention, and become one of the hottest research areas in China. This paper briefly reviews the progress and achievements related to QD lasers and inter sublevel QD photodetectors in China. Many interesting results have been made, but there are still challenges to acquire the excepted device performance.

Acknowledgment: The authors would like to thank Professor Q. Gong from Shanghai Institute of Micro system and Information Technology, CAS for providing the original figures regarding 1.55 μm QD lasers. This work is supported by "One-Hundred Talents Program" of the Chinese Academy of Sciences and the National Science Foundation of China (Nos. 60876033, 61076050, and 61021003).

References and Notes

1. O. Stier, M. Grundmann, and D. Bimberg, *Phys. Rev. B* 59, 5688 (**1999**).
2. A. J. Williamson, L. W. Wang, and A. Zunger, *Phys. Rev. B* 62, 12963 (**2000**).
3. H. Heidemeyer, C. M. Uller, and O. G. Schmidt, *J. Cryst. Growth* 261, 444 (**2004**).
4. V. M. Usinov, A. E. Zhukov, A. Y. Egorov, and N. A. Maleev, Quantum Dot Lasers, Oxford University Press Inc., New York (**2003**).
5. Y. Arakawa and H. Sakaki, *Appl. Phys. Lett.* 40, 939 (**1982**).
6. N. Kistaedter, N. N. Ledentsov, M. Grundman, D. Bimberg, U. Richter, S. S. Ruvimov, P. Werner, J. Heydenreich, V. M. Ustinov, M. V. Maximov, P. S. Kop'ev, and Z. I. Alferov, *Electron. Lett.* 33, 1150 (**1994**).
7. K. Sebald, P. Michler, T. Passow, D. Hommel, G. Bacher, and A. Forchel, *Appl. Phys. Lett.* 81, 2920 (**2002**).
8. M. B. Ward, O. Z. Karimov, D. C. Unitt, Z. L. Yuan, P. See, D. G. Gevaux, A. J. Shields, P. Atkinson, and D. A. Ritchie, *Appl. Phys. Lett.* 86, 201111 (**2005**).
9. W. Löffler, D. Tröndle, J. Fallert, H. Kalt, D. Litvinov, D. Gerthsen, J. Lupaca-Schomber, T. Passow, B. Daniel, J. Kvietková, M. Grün, C. Klingshirn, and M. Hetterich, *Appl. Phys. Lett.* 88, 062105 (**2006**).

10. Z. G. Wang, *Proceeding of the Fifth Chinese Conference on Solid Films*, Chengde, China, October **(1996)**.
11. Z. G. Wang, F. Q. Liu, J. B. Liang, B. Xu, D. Ding, Q. Gong, and Q. Han, *Chin. Journal of Semiconductors* 21, 827 **(2000)**.
12. H. Y. Liu, B. Xu, Y. Q. Wei, D. Ding, J. J. Qian, Q. Han, J. B. Liang, and Z. G. Wang, *Appl. Phys. Lett.* 79, 2868 **(2001)**.
13. H. D. Yang, Q. Gong, S. G. Li, C. F. Cao, C. F. Xu, P. Chen, and S. L. Feng, *J. Cryst. Growth* 312, 3451 **(2010)**.
14. H. Y. Liu, I. R. Sellers, R. J. Airey, M. J. Steer, P. A. Houston, D. J. Mowbray, J. Cockburn, M. S. Skolnick, B. Xu, and Z. G. Wang, *Appl. Phys. Lett.* 80, 3769 **(2002)**.
15. Z. C. Niu, H. Q. Ni, Z. D. Fang, Z. Gong, S. Y. Zhang, D. H. Wu, Z. Sun, H. Zhao, H. L. Peng, Q. Han, and R. H. Wu, *Chin. Journal of Semiconductors* 27, 482 **(2006)**.
16. H. M. Ji, T. Yang, Y. L. Cao, P. F. Xu, Y. X. Gu, W. Q. Ma, and Z. G. Wang, *Chin. Phys. Lett.* 27, 027801 **(2010)**.
17. Y. L. Cao, T. Yang, H. M. Ji, W. Q. Ma, Q. Cao, and L. H. Chen, *IEEE Photon. Technol. Lett.* 20, 1860 **(2008)**.
18. H. M. Ji, T. Yang, Y. L. Cao, P. F. Xu, Y. X. Gu, Y. Liu, L. Xie, and Z. G. Wang, *Chin. Phys. Lett.* 27, 034209 **(2010)**.
19. P. F. Xu, T. Yang, H. M. Ji, Y. L. Cao, Y. X. Gu, Y. Liu, W. Q. Ma, and Z. G. Wang, *J. Appl. Phys.* 107, 013102 **(2010)**.
20. S. G. Li, Q. Gong, Y. F. Lao, K. He, J. Li, Y. G. Zhang, S. L. Feng, and H. L. Wang, *Appl. Phys. Lett.* 93, 111109 **(2008)**.
21. S. G. Li, Q. Gong, Y. F. Lao, H. D. Yang, S. Gao, P. Chen, Y. G. Zhang, S. L. Feng, and H. L. Wang, *Appl. Phys. Lett.* 95, 251111 **(2009)**.
22. J. Wu, B. Xu, H. X. Li, Q. W. Mo, Z. G. Wang, X. M. Zhao, and D. Wu, *J. Cryst. Growth* 197, 95 **(1999)**.
23. H. X. Li, J. Wu, Z. G. Wang, and T. D. Race, *Appl. Phys. Lett.* 75, 1173 **(1999)**.
24. X. R. Yang, B. Xu, L. Y. Liang, C. G. Tang, Y. Y. Ren, X. L. Ye, and Z. G. Wang, *Nanotechnology* 18, 215302 **(2007)**.
25. X. R. Yang, B. Xu, Z. G. Wang, P. Jin, P. Liang, Y. Hu, H. Sun, Y. H. Chen, and F. L. Liu, *Electron. Lett.* 42, 757 **(2006)**.
26. D. Pan, Y. P. Zeng, M. Y. Kong, J. Wu, Y. Q. Zhu, C. H. Zhang, J. M. Li, and C. Y. Wang, *Electron. Lett.* 32, 18 **(1996)**.
27. W. Q. Ma, Y. W. Sun, X. J. Yang, D. S. Jiang, and L. H. Chen, *Nanotechnology* 17, 5765 **(2006)**.
28. W. Q. Ma, Y. W. Sun, X. J. Yang, M. Chong, D. S. Jiang, and L. H. Chen, *Infrared Phys. Technol.* 50, 162 **(2007)**.
29. W. Q. Ma, X. J. Yang, M. Chong, T. Yang, L. H. Chen, J. Shao, X. Lü, W. Lu, C. Y. Song, and H. C. Liu, *Appl. Phys. Lett.* 93, 013502 **(2008)**.
30. T. Yang, J. Tatebayashi, S. Tsukamoto, M. Nishioka, and Y. Arakawa, *Appl. Phys. Lett.* 84, 2817 **(2004)**.
31. O. B. Shchekin and D. G. Deppe, *Appl. Phys. Lett.* 80, 15 **(2002)**.
32. K. Otsubo, N. Hatoti, M. Ishida, S. Okumura, T. Akiyama, Y. Nakata, H. Ebe, M. Sugawara, and Y. Arakawa, *Jpn. J. Appl. Phys.* 43, 8B **(2004)**.
33. Y. L. Cao, T. Yang, P. F. Xu, H. M. Ji, Y. X. Gu, X. D. Wang, Q. Wang, W. Q. Ma, and L. H. Chen, *Appl. Phys. Lett.* 96, 171101 **(2010)**.
34. C. Paranthoen, N. Bertru, O. Dehaese, A. Le Corre, S. Loualiche, B. Lambert, and G. Patriarche, *Appl. Phys. Lett.* 78, 1751 **(2001)**.
35. Q. Gong, R. Nötzel, P. J. van Veldhoven, T. J. Eijkemans, and J. H. Wolter, *Appl. Phys. Lett.* 84, 275 **(2004)**.
36. Q. Gong, R. Nötzel, P. J. van Veldhoven, T. J. Eijkemans, and J. H. Wolter, *Appl. Phys. Lett.* 85, 1404 **(2004)**.
37. J. Liu, Z. Lu, S. Raymond, P. J. Poole, P. J. Barrios, and D. Poitras, *Opt. Lett.* 33, 1702 **(2008)**.
38. V. Ryzhii, *Semicond. Sci. Technol.* 11, 759 **(1996)**.

Received: 26 April 2011. Accepted: 2 June 2011.

REVIEW